Semiexclusive pionic double charge exchange on ^{4}He

J. L. Clark and M. E. Sevior
School of Physics, University of Melbourne, Parkville, Victoria 3052, Australia

H. Clement, J. Gräter, R. Meier, and G. J. Wagner
Physikalisches Institut, Universität Tübingen, Morgenstelle 14, D-72076 Tübingen, Germany

P.-A. Amaudruz, L. Felawka, G. J. Hofman, D. Ottewell, and G. R. Smith*
TRIUMF, 4004 Wesbrook Mall, Vancouver, British Columbia, Canada V6T 2A3

A. Ambardar, M. Kermani, and G. Tagliente
Physics Department, University of British Columbia, Vancouver, British Columbia, Canada V6T 2A6

P. Camerini, E. Fragiacomo, N. Grion, and R. Rui
University and INFN Trieste, I-34127 Trieste, Italy

E. L. Mathie,† R. Tacik, and D. M. Yeomans
University of Regina, Regina, Saskatchewan, Canada S4S 0A2

E. F. Gibson
California State University, Sacramento, California 95819

J. T. Brack
University of Colorado, Boulder, Colorado 80309

M. Schepkin
Institute for Theoretical and Experimental Physics, RU-117218 Moscow, Russia
(Received 12 July 2002; published 27 November 2002)

The semiexclusive reaction $^4\mathrm{He}(\pi^+,\pi^- pp)pp$ has been studied at pion kinetic energies of 105 MeV and 115 MeV. Signatures from the production of the hypothetical πNN resonance d' have been searched for in the invariant mass $M_{\pi pp}$ spectra. No hint for a dominant d' production, as anticipated from double charge exchange excitation functions on nuclei, has been found. The data are satisfactorily described by sequential single charge exchange.

DOI: 10.1103/PhysRevC.66.054606 PACS number(s): 25.80.Gn, 24.30.Gd, 14.20.Pt

I. MOTIVATION

Hadronic matter consists of two types of multiquark systems, $q\bar{q}$ and qqq. No well-established candidates for other ''exotic'' combinations, in particular confined six-quark systems (dibaryons), are known [1], although there have been numerous claims (see Ref. [2] for a review). Since the H particle was predicted by Jaffe [3] some 20 years ago, a large number of dibaryon calculations with QCD-inspired models have been carried out. Most experimental searches have focused on dibaryons with possible decays to the nucleon-nucleon (NN) or the nucleon-delta ($N\Delta$) system, where a very large decay width can be expected, which makes these states difficult to detect.

A narrow NN decoupled dibaryon has been suggested as the explanation of the peculiar behavior of the excitation function of the forward angle cross section in pionic double charge exchange (DCX) on nuclei [4]. For a wide range of nuclei, from ^{7}Li to ^{93}Nb, a dramatic peak of the cross section at low energies, around $T_\pi = 50$ MeV, has been found [4,5]. While there are attempts to describe this effect within the scope of conventional reaction mechanisms [6,7], the data are well described by the assumption of the formation of the so-called d' dibaryon. With a d' mass of $m = 2.06$ GeV, the narrow width of $\Gamma_{\pi NN} = 0.5$ MeV for decay to the πNN channel, and the quantum numbers $I(J^P) = \mathrm{even}(0^-)$, all measured DCX transitions can be reproduced reasonably well, both in their energy and their angular dependence. The small number of parameters in the d' model needed for a good description of DCX data on a wide variety of nuclei is very appealing. On the other hand, conventional calculations incorporating subtle medium effects may eventually provide a satisfactory explanation of the data. In fact, qualitative agreement has been achieved for a subset of the measured data within the framework of a conventional calculation without the need for a d' [7]. For a clear proof of the existence of the d', it is necessary to find

*Present address: Jefferson Lab, 12000 Jefferson Avenue, Newport News, VA 23606.
†Electronic address: mathie@uregina.ca

its signature in systems where medium effects are minimal or absent.

Possible production of the d' in vacuum has been suggested to occur in proton-proton collisions, in particular in the reaction $pp \rightarrow d'\pi^+ \rightarrow pp\pi^+\pi^-$ [8]. In this case, the d' signature is a peak at the mass of the dibaryon in the invariant mass spectrum of the $pp\pi^-$ system in the final state. Indeed, the WASA/PROMICE collaboration at the CELSIUS synchrotron has investigated this reaction and reported a 2–3 σ enhancement (depending on the treatment of the background) in the region of 2.06 GeV [9], which they interpreted as possible evidence for the d'. For verification, this measurement has been repeated and extended to another energy by the same group. The analysis of these data has been finished recently. At the level of 3σ statistical significance, no signal of the d' was found [10].

When pursuing the search for the d' in DCX, one has to use light target nuclei such as the helium isotopes to minimize medium effects. DCX on these nuclei does not lead to discrete final states but to a continuum of unbound identical nucleons. Signatures for the d' in the inclusive total DCX cross section on helium isotopes have been predicted by Clement *et al.* [11]. Production of the d' should lead to a significant enhancement of the cross section just above the d' threshold. An experiment performed with the CHAOS detector at TRIUMF has reported results for inclusive total DCX cross sections on ^{4}He [12]. The measured excitation function is consistent with the prediction from the d' model, although the conclusions are weakened by the strong model dependence of the description of the conventional DCX background.

Here we present the results from an alternative search for the d' in DCX on ^{4}He. If the DCX proceeds via an intermediate state that includes the formation of the d', i.e., $\pi^+ {}^4\mathrm{He} \rightarrow d'pp \rightarrow \pi^- pppp$, the π^- and two of the protons in the final state come from the d' decay. Thus the d' should show up as a peak at $m_{d'}$ in the invariant mass spectrum of the three detected particles, independent of the bombarding energy. This method of testing the d' hypothesis is less model dependent than the more usual approaches, which compare data to calculations with and without additional d' parameters. Such approaches lead invariably to better descriptions with the additional degrees of freedom provided by the d' parameters, but do not really provide firm evidence for the d'. In this experiment, the presence of a peak in the $\pi^- pp$ invariant mass spectrum at the predicted d' mass independent of bombarding energy would constitute model independent proof of the existence of the d'.

The invariant mass distribution ($M_{\pi^- pp}$) for the reaction $^4\mathrm{He}(\pi^+, \pi^- pp)pp$ was measured for incident pion energies of 105 MeV and 115 MeV, respectively 25 and 35 MeV above the d' production threshold. The energies were chosen as the best trade-off between (i) distinguishing the d' peak from the conventional DCX distribution and (ii) gaining a large enough d' contribution over the nonresonant DCX background. The former is not possible near threshold where the conventional background has a very narrow phase-space distribution. The latter criterion is only satisfied sufficiently close to threshold [11]. The d' hypothesis predicts a significant peak in the invariant mass distributions.

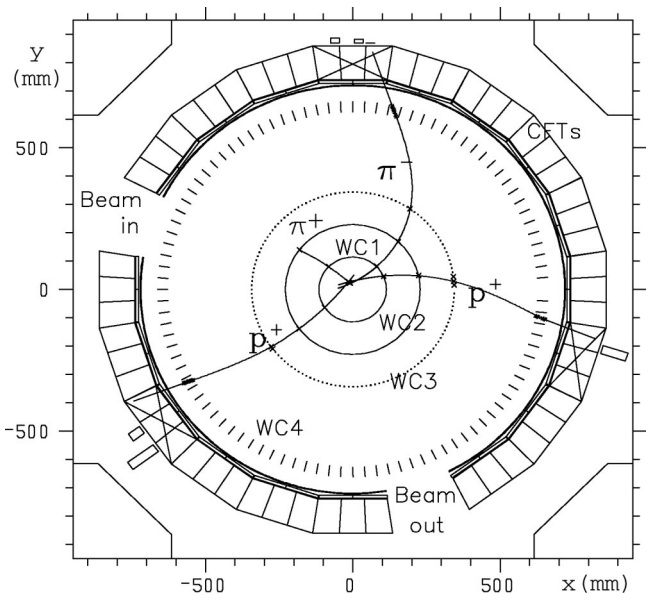

FIG. 1. A typical DCX event in which two protons were detected in plane with the outgoing π^-. The pion beam enters from the left and is detected in the inner two chambers only. The gas target occupies the entire inner volume of WC1. The rectangles behind the CFTs indicate energy losses in the $\Delta E1$ and $\Delta E2$ scintillators.

In this paper we give a description of the experiment (Sec. II), data analysis techniques (Sec. III), discussion of the results including model predictions (Sec. IV), and finally our conclusions (Sec. V).

II. EXPERIMENT

The search was conducted using the CHAOS spectrometer [13] in the $M11$ channel at TRIUMF. The spectrometer consists of low mass, cylindrical tracking chambers and particle identification counters immersed in a vertical magnetic field provided by a cylindrical dipole magnet. Radially outwards from the center are two proportional vertex wire chambers (WC1,WC2), a drift chamber (WC3 [14]), and, in the tail of the magnetic field, a vector drift chamber (WC4). Surrounding the WC4 detector are two layers of plastic scintillation counters ($\Delta E1$ and $\Delta E2$) and an outer layer of lead-glass Cerenkov counters, arranged in 18 separate blocks. These counters form the first-level CHAOS fast trigger [15] (CFT) and provide pion and proton particle identification during the off-line analysis. The distance from the center of the detector to the CFT's is about 70 cm. A schematic diagram is shown in Fig. 1. Charged particles were accepted over 360° in the scattering plane (except for 18° wide holes in the regions of the incoming and outgoing beam), and within $\pm 7°$ out of plane. Since π^+ fluxes of ~ 1 MHz were employed in this experiment, in the regions of the incoming and outgoing beam the low rate capability drift chambers WC3 and WC4 were deadened and the corresponding CFT blocks removed. Information on the out-of-plane track coor-

dinates was obtained from inclined cathode pickup strips in chambers WC1 and WC2. In this experiment additional pion-proton particle identification was achieved by analyzing the pulse heights from these strips.

As the protons from the DCX reaction have low energies and would not emerge from a liquid cryogenic target, a ^{4}He gas target at standard temperature and pressure was used. A constant flow of He gas filled the space within WC1. This defined a cylindrical target volume of radius 11 cm and height 10 cm. The gas volume was separated from the chamber walls by a 25-μm aluminized Mylar foil followed by a 0.5-cm-thick nitrogen flushing volume and sealed on top and underneath by aluminum plates attached to the frame of the wire chamber. The helium gas outflow was monitored for oxygen contamination to detect leaks and to verify the purity of the target gas.

A sophisticated multilevel trigger was used to filter the event stream. The first-level trigger was determined by the signal from an in-beam scintillation counter ($S1$) located at the beam entrance of the spectrometer, a $\Delta E1_i$ signal from any one or more CFT blocks as well as a negated signal from a veto counter (V) at the beam exit: $S1 \cdot \Delta E1_i \cdot \overline{V}$. This relatively loose (singles) trigger required only the pion to reach the outer detectors but included events where higher-energy protons (also) reached the CFTs.

The second-level trigger [16] employed hit information from the inner wire chambers (WC1, WC2, and (for most calculations) WC3) to evaluate the momentum, scattering angle, and polarity of the outgoing tracks. Since many of the low-energy protons produced in DCX stopped before penetrating WC3, the second-level trigger was programmed to require a triple coincidence by demanding a negative polarity outgoing track (searching for the π^-) and at least two non-adjacent additional hits in each of the chambers WC1 and WC2 within a certain angular range (searching for the two protons).

In addition to the DCX data at $T_\pi = 105$ and 115 MeV, some $\pi^+ p$ elastic scattering data using an argon/isobutane gas target were acquired to assist in calculating the particle energy losses and the efficiencies of the various detectors.

III. ANALYSIS

In all, about 200 million events were recorded at 115 MeV, and about 100 million events at 105 MeV. Particle identification for tracks reaching the trigger counters was performed by comparing the track momentum with the pulse height from the $\Delta E1$ scintillators. This provided reliable discrimination between pions and protons ($\geqslant 99\%$).

Identifying the low-energy tracks that stopped before reaching the $\Delta E1$ counters (42% of proton tracks found) was achieved by using the digitized pulse heights from the cathode strips in the inner two-wire chambers. Using regions defined in a scatterplot of pulse height versus the particle momentum, a proton identification efficiency of 94% was achieved. Positive particle identification required an unambiguous signal from both inner wire chambers.

Approximately 17% of proton tracks found did not have enough energy to arrive at the third wire chamber. These tracks had only two wire chamber hits to reconstruct the trajectory and were therefore momentum analyzed using the reaction vertex as a third point. The reaction vertex was determined from the intersection of the incoming π^+ track and the other outgoing tracks. When more than one outgoing track was available, an average vertex position was constructed. This average used a heavier weight for the tracks most perpendicular to the incoming beam. The typical vertex resolution in the scattering plane was 2.5 mm (σ).

Due to the loose first- and second-level trigger requirements, the vast majority of recorded events were due to noise in the wire chamber electronics. Off-line track sorting, kinematic cuts, and particle identification reduced the dataset to about 1000 events. The majority of the remaining background was due to DCX reactions in the walls of the target (the inner wire chamber) and back scattering of beam particles from a wire chamber wall, producing the illusion of a DCX event. Once these background events were removed, 157 and 64 DCX events were found at 115 and 105 MeV, respectively. A typical DCX event in CHAOS is shown in Fig. 1.

In order to form a more accurate $M_{\pi pp}$ invariant mass, corrections were made to account for the energy loss of particles as they traversed the detector material. These corrections were calculated using the $\pi^+ p$ elastic scattering data. The momentum calculated for the pion and proton tracks was compared with the ''true'' momentum at the interaction vertex as calculated from the known incident momentum, pion scattering angle, and two-body kinematics. This procedure showed that the momenta of particles traversing all four wire chambers were determined to within 5% ($\delta p/p$). However, it was found that this technique led to inaccurate results for low-energy tracks that stopped before WC4. Instead, different relationships between the vertex and measured momenta were determined for tracks that reached only WC3 and for tracks that only reached WC2. The $\pi^+ p$ elastic scattering data were also used for this analysis. In the latter case, the momenta considered were so low that the distance that the particle traveled within the target was also taken into account. This was not necessary for the other cases. $\Delta p/p$ for these short tracks was about 7%.

The invariant mass distributions were calculated according to the definition

$$M^2 = \left(\sum_{i=1}^{n} E_i \right)^2 - \left(\sum_{i=1}^{n} \vec{P}_i \right)^2 .$$

For the $M_{\pi pp}$, distribution, the summation includes the scattered pion and two detected protons, and for M_{pp} it includes just two protons. Using energy-momentum conservation, the missing energy (E_{miss}) and momentum (P_{miss}) associated with the two protons not detected in the event can also be calculated. This allows a second determination (we call this the ''reverse invariant mass'') of $M_{\pi pp}^{Rev}$ using

$$(M_{\pi pp}^{Rev})^2 = (E_{\pi^-} + E_{\mathrm{miss}})^2 - (\vec{P}_{\pi^-} + \vec{P}_{\mathrm{miss}})^2 .$$

More details on the data analysis are available in Ref. [17].

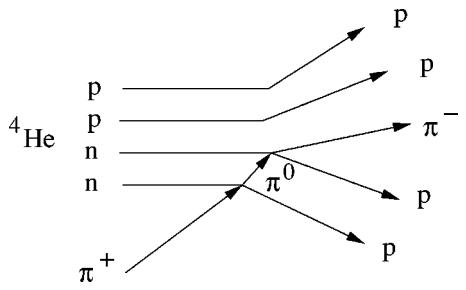

FIG. 2. Graph of DCX process proceeding via SSCX.

IV. RESULTS AND DISCUSSION

A. Models

Two models were considered for our simulations. The conventional model is based on sequential single charge exchange (SSCX; Fig. 2), of which there are several theoretical implementations [18–22]. In our version, an on-shell Monte Carlo model [12] was used. Random Fermi momenta extracted from existing ^{4}He$(e,e'$p) data were initially assigned to the four nucleons in ^{4}He. The neutrons were then involved in two consecutive two-body SCX reactions, $n(\pi^+,\pi^0)p$ and $n(\pi^0,\pi^-)p$, resulting in a final state of a π^- and four protons. The SCX reactions were weighted according to the experimental cross sections for πN SCX extracted from the SM95 solution of the SAID database [23]. It was assumed that all the energy required to break up the ^{4}He nucleus was lost in the first step [12] and that all the intermediate particles were on shell.

The graph for the resonant DCX process, i.e., with the d' in the intermediate state, is shown in Fig. 3. Calculations were performed in order to predict the fraction of DCX reactions occurring through the resonant channel [8] and applied to ^{4}He [11]. The d' contribution was expected to account for about 50% of the total DCX cross section at our energies, using the on-shell SSCX model, and about 90% using the Gibbs-Rebka model [21,24] as the background process. To predict spectra of observables, a d' Monte Carlo model was used. In this calculation the formation of a resonance with a mass of 2.06 GeV and a width of 0.5 MeV from the incoming pion and the two neutrons was assumed. Phase space was used for the distribution of the d' and the two remaining protons. Since the maximum kinetic energy of the d' decay protons is only 20 MeV, final-state interaction (FSI) effects [25,26] are expected to influence the decay mechanism. Our d' Monte Carlo model incorporated FSI effects following the approach in Ref. [8], which biased the d' protons to states of low relative momentum.

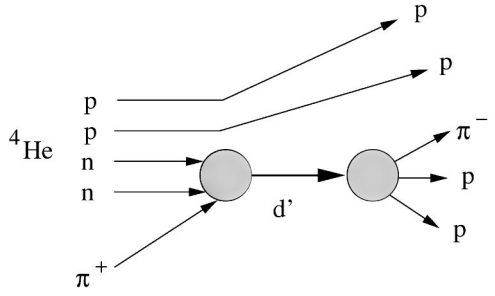

FIG. 3. Graph of DCX process proceeding via the d' mechanism.

Both models were used as event generators in the GEANT [27] detector simulation package. The resulting kinematic observables incorporate the CHAOS acceptance and resolution and can be directly compared to those extracted from the experimental data. The resulting invariant mass resolution was 8 MeV.

B. Results

The top two histograms in Fig. 4 show the results for the invariant mass spectra calculated from the momenta of the detected π^- and two protons, as well as the predictions from the two-model simulations. The normalization was obtained using a least-squares fit. For the d' mechanism, shown as the solid double line, a peak at the invariant mass of the d' is expected. However, since there are four protons in the final state, the peak is accompanied by a combinatorial background resulting from detecting one or two of the protons that are not from the d'. Nonresonant DCX, modeled as SSCX as described above, produces a continuous distribution of the invariant mass, shown by the solid single line. The dotted line shows curves for five-body phase space. The data points are shown with statistical error bars only, which are those used for small signals and tabulated in Ref. [28].

To extract the relative contributions of the SSCX and the d' mechanisms necessary to describe the data, the invariant mass spectra were fit with the curves from the simulation. In this fit, the relative contribution of the SSCX and d' were left as free parameters. The curves were corrected for the slightly different detector acceptances appropriate for the two mechanisms. From this least-squares fit, the fraction of events attributed to each mechanism was found. Results of the fits are summarized in Table I.

For the 115-MeV $M_{\pi pp}$ data, no d' contribution was required in the best fit, but a d' fraction of 0.34 was allowed at 90% confidence level. The 105-MeV data required a dibaryon contribution of 0.04 in the best fit. However, at this energy the $M_{\pi pp}$ data could hardly distinguish between the models at 90% confidence level. In both cases, the reduced χ^2 for the SSCX mechanism was significantly better than for the d' mechanism.

The distribution of $M_{\pi pp}^{Rev}$ is shown in the middle histograms in Fig. 4. Again, the SSCX model adequately explains the data at both energies. It is advantageous to use the reverse invariant mass distribution for the 105-MeV data because the peak of the background (conventional) process is further away from the d' peak. A tighter limit may be placed on d' production: a d' contribution of 0.01 was required in the best fit, and up to 0.39 allowed at the 90% confidence limit. Also here, the better description of the data by the SSCX model compared to the d' model leads to a significantly better reduced χ^2.

The invariant mass of the two observed protons is also shown (bottom spectra in Fig. 4), providing a measure of the FSI of the d' decay, which would cause the decay protons to tend to a small relative momentum and result in a peak at

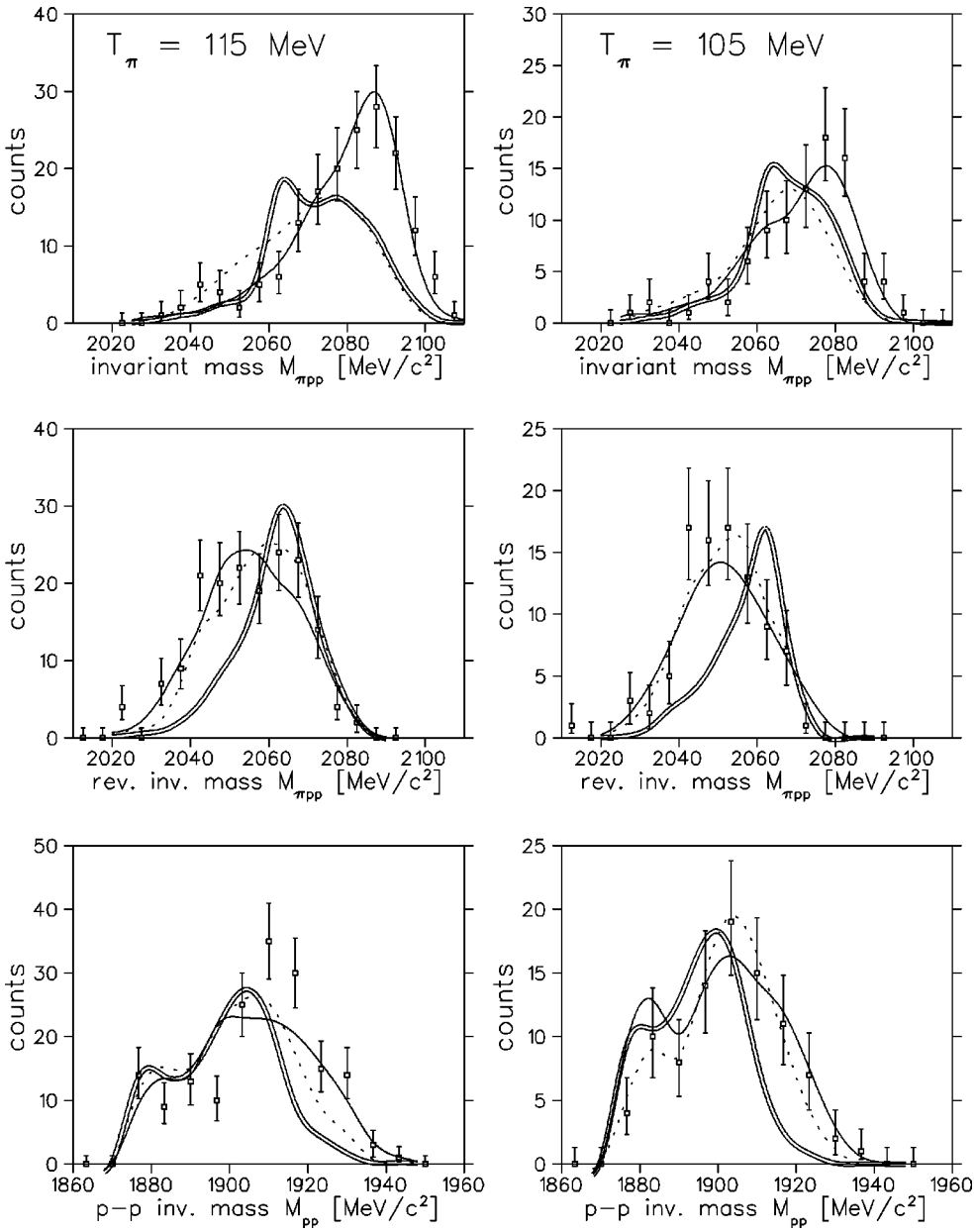

FIG. 4. The invariant mass of the observed pion and two protons is shown in the top histograms, the "reverse" invariant mass in the middle histograms, and the invariant mass of the two protons in the bottom histograms. The histograms on the left are for $T_\pi = 115$ MeV and those on the right are for $T_\pi = 105$ MeV. The lines show simulation results from the dibaryon mechanism (double solid line), the conventional (SSCX) mechanism (single solid line), and five-body phase space (dotted line). Error bars are statistical only and have been calculated according to Ref. [28].

low invariant mass. At both energies the SSCX mechanism performs significantly better than the dibaryon mechanism.

The d' does not make a significant contribution in the best fit in any of the graphs. The SSCX with FSI model adequately describes all the data with the exception of the proton-proton invariant mass histogram at $T_\pi = 115$ MeV, but here the d' does not improve the situation.

Recently it has been questioned whether the d' predictions in Ref. [11] have been grossly overestimated due to the underestimation of the collision damping $d'N \rightarrow NNN$ [29]. The latter process is taken into account in the d' model by a spreading width Γ_s where the value $\Gamma_s = 5$ MeV had been derived from the initial d' analysis of DCX data [4]. A more recent analysis of high-quality DCX data for $7 \leqslant A \leqslant 93$ yields a significantly higher value [5] $\Gamma_s \sim 10$–20 MeV with $\Gamma_s = 15$ MeV for $A = 7$, the closest neighbor of the He cases. The consequences of an increased spreading width would be severe. It would lead to a reduction by up to a factor of 40 of the predicted d' cross sections. In addition, the increased total d' width of $\Gamma \sim \Gamma_s \sim 15$ MeV would be substantially larger than the experimental resolution of $\Delta M_{\pi pp} \sim 8$ MeV. The d' peak in the spectrum would be washed out, diminishing the shape differences between d' and conventional spectra.

TABLE I. Results of dibaryon search showing the calculated reduced χ^2 values for the fits of the data to the two competing models, as well as the d' contribution for the combination of the two models, which produces the lowest χ^2 value, and the d' contribution upper limit at the 90% confidence level. These values are tabulated for the three different observables: the invariant mass $M_{\pi pp}$, the ''reverse'' invariant mass $M_{\pi pp}$ (rev), and the invariant mass of the two protons, M_{pp}.

	115 MeV				105 MeV			
	Reduced χ^2		d' fraction		Reduced χ^2		d' fraction	
	SSCX	d'	Best fit	90% C.L.	SSCX	d'	Best fit	90% C.L.
$M_{\pi pp}$	0.7	5.0	0.00	0.34	0.8	1.6	0.04	0.92
$M_{\pi pp}$ (rev)	1.2	3.9	0.12	0.42	0.9	3.4	0.01	0.39
M_{pp}	2.2	5.2	0.00	0.00	0.6	3.0	0.00	0.53

V. CONCLUSIONS

The DCX reaction on ^{4}He has been studied semiexclusively with the CHAOS spectrometer by detecting two of the four outgoing protons in addition to the outgoing negative pion. The resulting invariant mass spectra exhibit new, detailed information on the reaction mechanism. The data for $M_{\pi pp}$ and M_{pp}, which are particularly well suited to search for signatures of a possible d' production, indicate that the contribution of the d' mechanism is substantially smaller than that predicted in Ref. [11] and that anticipated from the analysis of the total cross sections in Ref. [12]. The SSCX Monte Carlo simulations describe the new experimental data satisfactorily, without requiring even a small d' contribution.

ACKNOWLEDGMENTS

We gratefully acknowledge the assistance provided by the technical and support staff of TRIUMF. This work was supported by the German Federal Minister of Education and Research (BMBF) under Contract No. 06TU887/987 and by the Deutsche Forschungsgemeinschaft (Graduiertenkolleg Grant No. MU705/3). It received further support from the National Science and Engineering Research Council (NSERC) of Canada, from the Instituto Nazionale di Fisica Nucleare (INFN), Italy, the Australian Research Council, and the California State University Sacramento Foundation.

[1] Particle Data Group, D.E. Groom *et al.*, Eur. Phys. J. C **15**, 1 (2000).
[2] K. K. Seth, in *Proceedings of the Conference on Medium and High Energy Nuclear Physics, Taiwan, 1988*, edited by W. Y. P. Hwang *et al*. (World Scientific, Singapore, 1989).
[3] R.L. Jaffe, Phys. Rev. Lett. **38**, 195 (1977).
[4] R. Bilger *et al.*, Z. Phys. A **343**, 491 (1992); Phys. Rev. Lett. **71**, 42 (1993).
[5] K. Föhl *et al.*, Phys. Rev. Lett. **79**, 3849 (1997); J. Pätzold *et al.*, Phys. Lett. B **428**, 18 (1998); **443**, 77 (1998).
[6] M.A. Kagarlis and M.B. Johnson, Phys. Rev. C **73**, 38 (1994).
[7] M. Nuseirat, M.A.K. Lodhi, M.O. El-Ghossain, W.R. Gibbs, and W.B. Kaufmann, Phys. Rev. C **58**, 2292 (1998).
[8] M. Schepkin, O. Zaboronsky, and H. Clement, Z. Phys. A **345**, 407 (1993).
[9] W. Brodowski *et al.*, Z. Phys. A **355**, 5 (1996).
[10] W. Brodowski *et al.*, Phys. Rev. Lett. **88**, 192301 (2002); nucl-ex/0206020, Phys. Lett. B (submitted).
[11] H. Clement, M. Schepkin, G.J. Wagner, and O. Zaboronsky, Phys. Lett. B **337**, 43 (1994).
[12] J. Gräter *et al.*, Phys. Lett. B **420**, 37 (1998); Phys. Rev. C **58**, 1576 (1998).
[13] G.R. Smith *et al.*, Nucl. Instrum. Methods Phys. Res. A **362**, 349 (1995).
[14] G.J. Hofman, J.T. Brack, P.A. Amaudruz, and G.R. Smith, Nucl. Instrum. Methods Phys. Res. A **325**, 384 (1993).
[15] F. Bonutti, S. Buttazzoni, P. Camerini, N. Grion, and R. Rui, Nucl. Instrum. Methods Phys. Res. A **350**, 136 (1994).
[16] K. Raywood, P.A. Amaudruz, S. McFarland, M.E. Sevior, and G.R. Smith, Nucl. Instrum. Methods Phys. Res. A **357**, 296 (1995).
[17] J. Clark, Ph.D. thesis, University of Melbourne, 2000.
[18] F. Becker and C. Schmidt, Nucl. Phys. **B18**, 607 (1970).
[19] R.I. Jibuti and R.Y.A. Kezerashvili, Nucl. Phys. **A437**, 687 (1985).
[20] J.F. Germond and C. Wilkin, Lett. Nuovo Cimento **13**, 605 (1975).
[21] W.R. Gibbs *et al.*, Phys. Rev. C **15**, 1384 (1977).
[22] J. Hüfner and M. Thies, Phys. Rev. C **20**, 273 (1979).
[23] R.A. Arndt, I.I. Strakovsky, R.L. Workman, and M.M. Pavan, Phys. Rev. C **52**, 2120 (1995).
[24] G. Rebka (private communication).
[25] K.W. Watson, Phys. Rev. **88**, 1163 (1952).
[26] A.B. Migdal, JETP **1**, 2 (1955).
[27] S. Giani *et al.*, computer code GEANT (CERN program library, Geneva, 1995).
[28] G.J. Feldman and R.D. Cousins, Phys. Rev. D **57**, 3873 (1998).
[29] J. Gräter *et al.*, Phys. Lett. B **471**, 113 (1999).